SUPPLEMENTARY INFORMATION

TITLE:

Structural Basis of Signal Sequence Surveillance and Selection by the SRP-SR Complex

AUTHORS and AFFILIATIONS

Ottilie von Loeffelholz[1,2], Kèvin Knoops[1,2,6], Aileen Ariosa[3,6], Xin Zhang[3,4], Manikandan Karuppasamy[1,2], Karine Huard[1,2], Guy Schoehn[1,2,5], Imre Berger[1,2], Shu-ou Shan[3*], Christiane Schaffitzel[1,2*]

[1] European Molecular Biology Laboratory, Grenoble Outstation, 6 Rue Jules Horowitz, BP181, 38042 Grenoble Cedex 9, France

[2] Unit of Virus Host-Cell Interactions, UJF-EMBL-CNRS, UMI 3265, 6 Rue Jules Horowitz, 38042 Grenoble Cedex 9, France

[3] Division of Chemistry and Chemical Engineering, California Institute of Technology, 1200 E. California Blvd, Pasadena, CA 91125, United States

[4] Department of Molecular and Experimental Medicine, The Scripps Research Institute, 10550 North Torrey Pines Road, La Jolla, CA 90037, United States

[5] CNRS / CEA/ UJF-Grenoble-1 - Institut de Biologie Structurale-Jean-Pierre Ebel, UMR 5075 41, rue Jules Horowitz, 38027 Grenoble Cedex, France

[6] These authors contributed equally to this work.

* Correspondence should be addressed to: S. S., *sshan@caltech.edu*; C. S., *schaffitzel@embl.fr*.

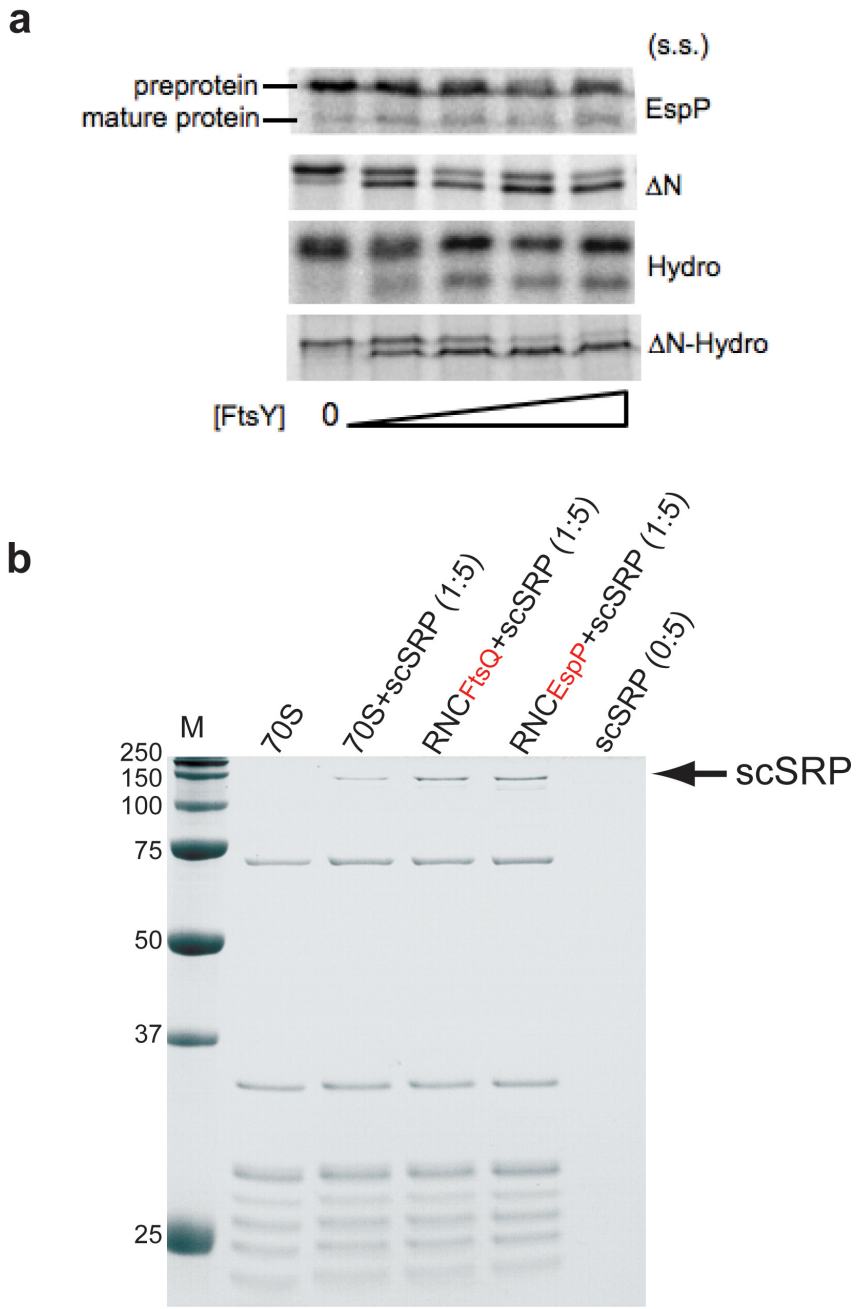

Supplementary Figure 1: ***In vitro*** **translocation of EspP signal sequence variants and SRP binding to ribosomal complexes. (a)** *In vitro* co-translational targeting and translocation through microsomal membranes. The EspP signal sequence variants were fused N-terminally to the signal peptidase cleavage site and to the mature region of pre-Prolactin. Translocation of the preprotein leads to cleavage of the signal sequence. **(b)** Coomassie-stained SDS-PAGE gel showing binding of single-chain SRP (scSRP) to 70S, RNC^{FtsQ}, and RNC^{EspP} analyzed by ribosomal pelleting. The protein band corresponding to scSRP is highlighted by an arrow. In all experiments, except the 70S control, ribosomes were incubated with a five-fold molar excess of scSRP in the absence of nucleotides.

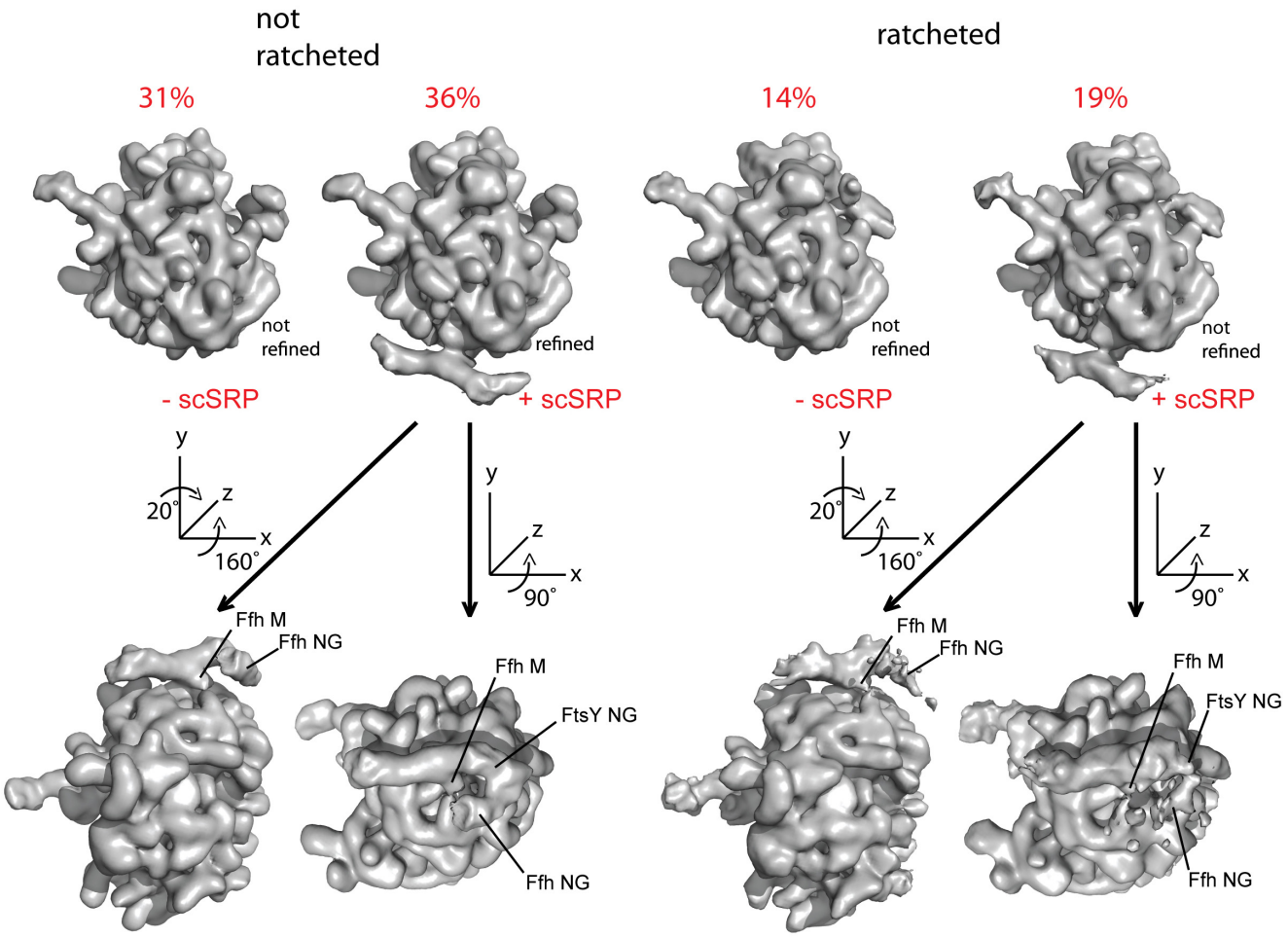

Supplementary Figure 2: **Computational Sorting of the RNC^{EspP}-SRP-FtsY data set.** The dataset was sorted for compositional and conformational heterogeneity to obtain four subgroups: Particles were separated for the ratcheted (EMDB ID 1363[56]) and for the not-ratcheted ribosome conformation (EMBD ID 1056[57]) as well as for the presence and the absence of SRP and FtsY (scSRP) at the exit of the ribosomal tunnel. **Upper row**: resulting maps after computational sorting [44]. **Second row**: Additional views of the non-ratcheted (left) and ratcheted (right) RNC^{EspP}-SRP-FtsY complexes. The first view (1st and 3rd image) on the ribosomal tunnel exit shows a second connection of the SRP to the ribosome formed by the Ffh M-domain. The second view (2nd and 4th image) is on the exit of the ribosomal tunnel and the SRP-FtsY complex. Both SRP-FtsY containing maps have a second ribosomal connection formed by the M-domain (second row, 1st and 3rd image) and a non-symmetric NG-domain arrangement. The map of the not ratcheted RNC^{EspP}-SRP-FtsY conformation corresponding to 36% of the dataset was refined to higher resolution.

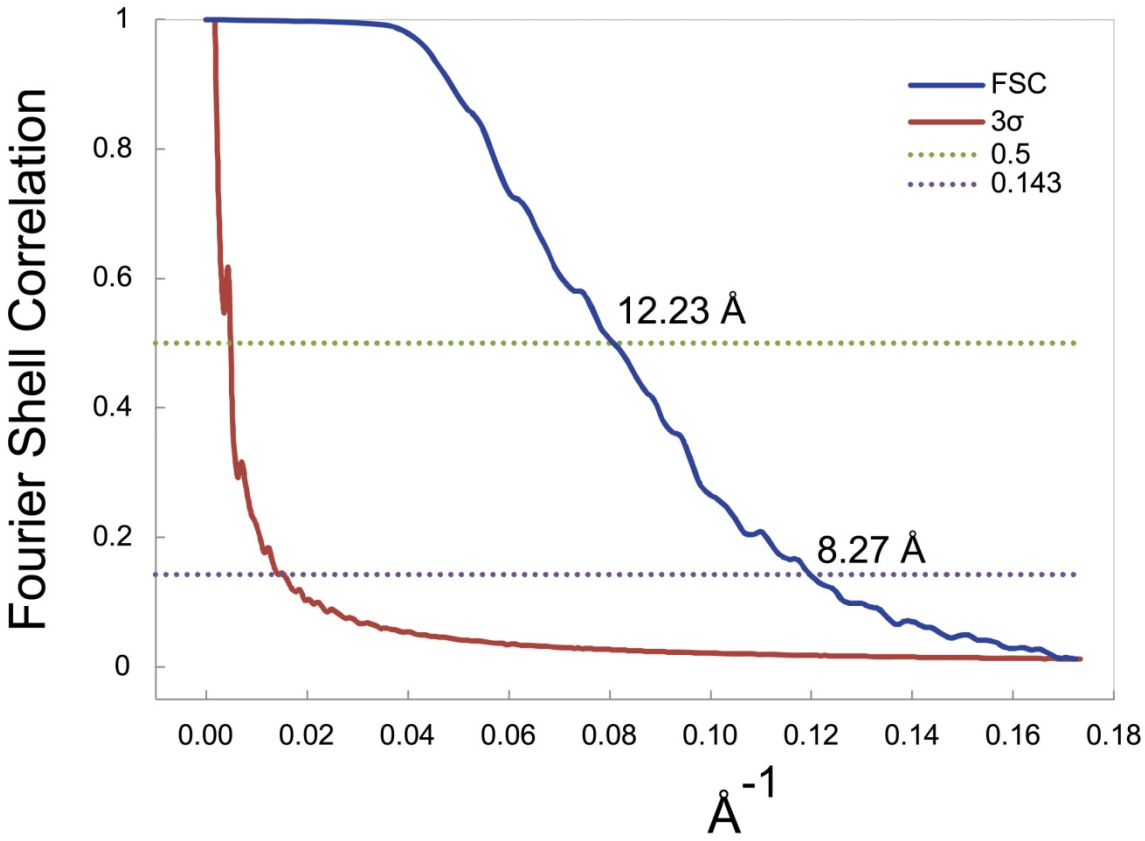

Supplementary Figure 3: **Resolution of the RNC^{EspP}-SRP-FtsY reconstruction.** The FSC function was calculated between two independent three-dimensional reconstructions of the RNC^{EspP}-SRP-FtsY complex (continuous blue line). A set of 46,945 particles was split randomly into two equal halves to calculate the two reconstructions. FSC=0.5 indicates a resolution of 12.2 Å (dotted green line), and FSC=0.143 [56] indicates a resolution of 8.3 Å (dotted purple line).

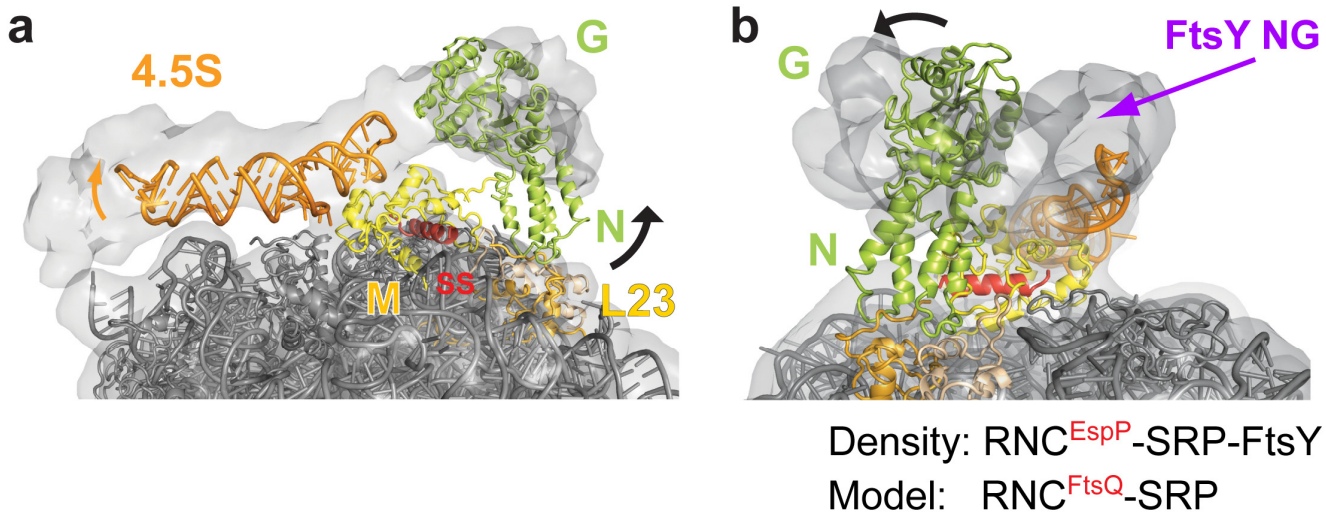

Supplementary Figure 4: **Conformational rearrangements of the targeting complex assessed by placement of the the RNC^{FtsQ}-SRP atomic model into the EM density of the 'false' *early* complex. (a,b)** The atomic model of the *E. coli* SRP bound to the translating ribosome (PDB ID: 2J28)[17] was placed into the EM density. Conformational changes of the Ffh NG-domain leading to a detachment from ribosomal protein L23 are indicated by black arrows. The detachment of the 4.5S RNA from the ribosomal protein L32 of the large ribosomal subunit is indicated by an orange arrow. The position in the EM density where the FtsY NG-domain is placed is highlighted by a purple arrow. The experimental density is depicted in light grey, 4.5S RNA in orange, the signal sequence in red, the Ffh M-domain in yellow, the Ffh NG-domain in greenyellow, the 50S rRNA in dark gray, L29 in wheat and L23 in orange.

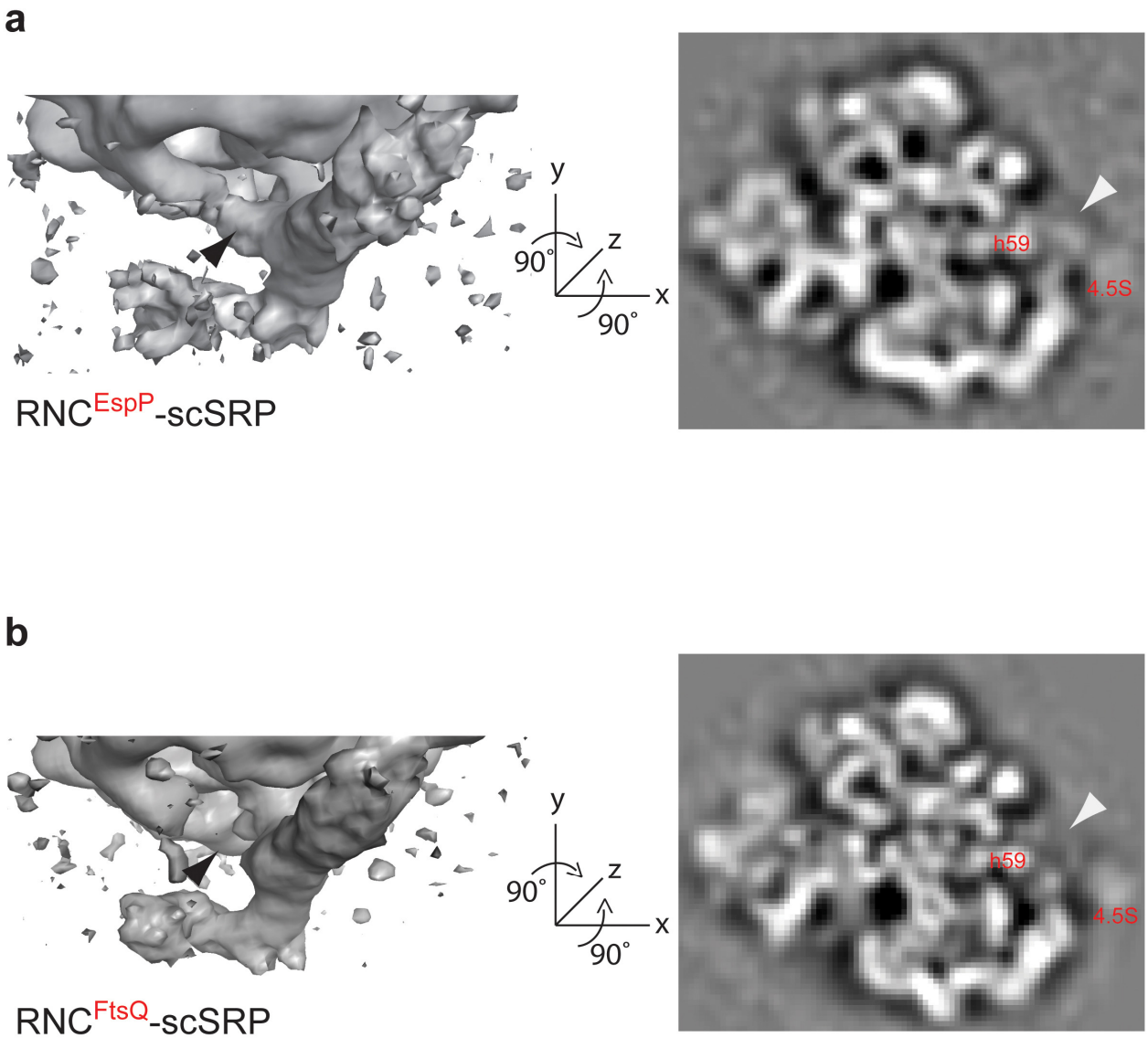

Supplementary Figure 5: Comparison of (a) the M-domain in the RNC^{EspP}-SRP-FtsY 'false' *early* complex and (b) the M-domain in the RNC^{FtsQ}-SRP-FtsY *early* complex (EMDB ID: 1762)[20]. Left: Close-up on the exit of the ribosomal tunnel and the M-domain of the RNC-SRP-FtsY complex in a surface representation. **Right:** Slice through the RNC-SRP-FtsY EM reconstruction. Ribosomal RNA helix h59 and the 4.5S SRP RNA are labelled for orientation. The arrow heads indicate the position of the signal-sequence binding part of the M-domain.

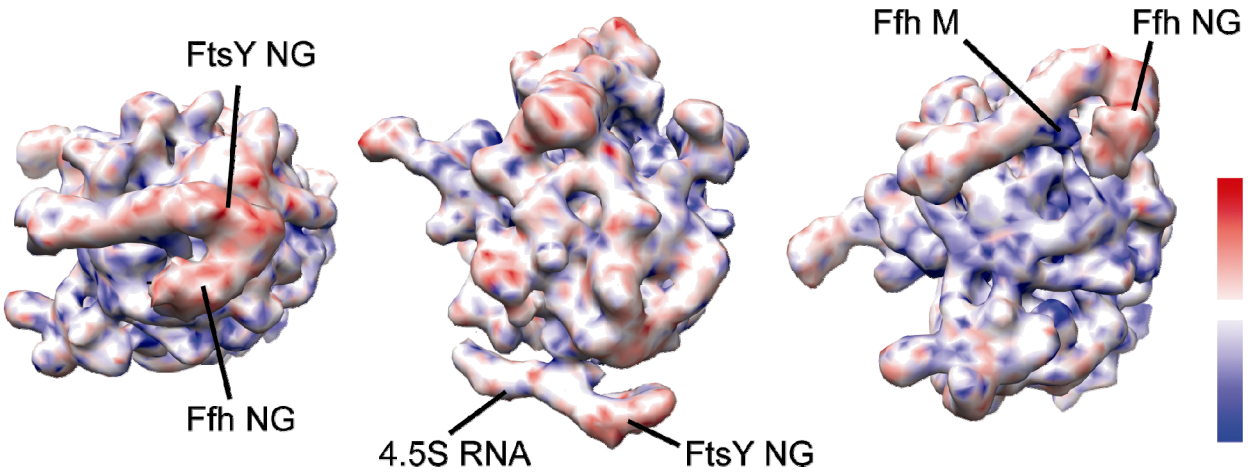

Supplementary Figure 6: Variance map of the RNC^{EspP}-SRP-FtsY reconstruction calculated from hypergeometrically stratified resampled volumes in SPARX. After elimination of particles with low correlation coefficient, 45,200 particles were used for the hypergeometrically stratified resampling to calculate the 3D average- and variance maps[58]. **Left:** view on the ribosomal tunnel exit site of the 50S and the SRP-FtsY complex; **middle:** crown view with the SRP-FtsY complex; **right:** view on the ribosomal tunnel exit showing the second connection of the SRP to the ribosome formed by the Ffh M-domain. Highly homogeneous regions (lower voxel variances) are coloured in blue, flexible or heterogeneous regions (higher voxel variances) are displayed in red. The surface representations were prepared in Chimera[59].

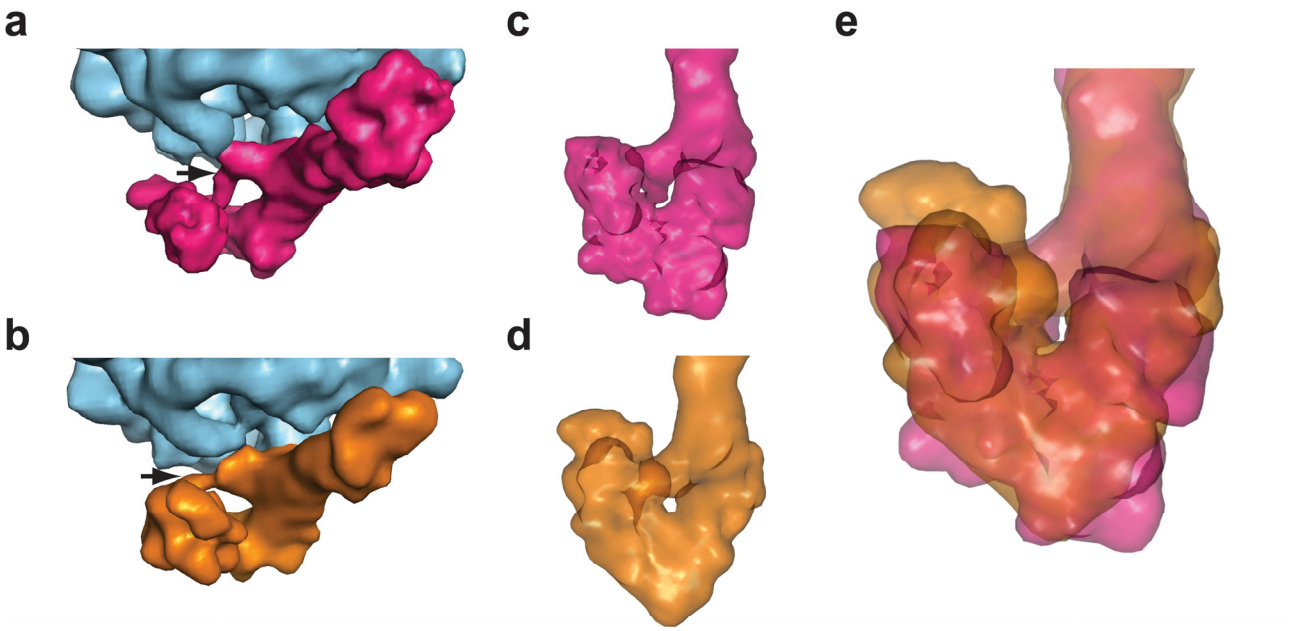

Supplementary Figure 7: **Two different conformations of the 'false' *early* complex obtained by heterogeneity analysis using Xmipp. (a,b)**: A heterogeneity analysis using mlf_refine3d from Xmipp[57] resulted in two EM reconstructions showing distinct conformations of the SRP-FtsY complex. In both EM reconstructions, the M-domain contacts rRNA helix 59. Arrows point to the connecting density between the Ffh G- and M- domains. **(c,d)** The EM density reveals two different Ffh/FtsY NG-domain conformations. **(e)** Overlay of the two maps shown in (c) and (d). In both conformations, the Ffh NG-domain is shifted towards the M-domain, and the NG-domains do not adopt a pseudo-symmetric V-shape.

	SRP Binding K_d (nM)	Early Complex K_d (nM)	Early – Closed Rearrangement k_{e-c} (s^{-1})	Closed Complex Assembly $k_{on} \times 10^3$ ($M^{-1}s^{-1}$)
RNC^{EspP} [1]	13	311	0.04 ± 0.01	9.2 ± 1.1
RNC^{FtsQ} [2]	1	80	~ 2	~ 1000

Supplementary Table 1: Comparison of kinetic and thermodynamic data of EspP as a non-SRP substrate with FtsQ as a *bona-fide* SRP substrate.

[1] Data from this study as reported in Figures 1d, 2b and 5c.

[2] The data for the RNC^{FtsQ} targeting complexes were originally reported in Zhang, X., Schaffitzel, C., Ban, N. & Shan, S.O. Multiple conformational switches in a GTPase complex control co-translational protein targeting. *Proc. Natl. Acad. Sci. USA* **106**, 1754-1759 (2009).